Article

An Innovative Trombe Wall for Winter Use: The Thermo-Diode Trombe Wall

Jerzy Szyszka [1] **, Piero Bevilacqua** [2,*] **and Roberto Bruno** [2]

[1] Faculty of Civil and Environmental Engineering and Architecture, Rzeszow University of Technology, 35-959 Rzeszów, Poland; jszyszka@prz.edu.pl

[2] Department of Mechanical, Energetic and Management Engineering, University of Calabria, Arcavacata di Rende, 87036 Cosenza, Italy; roberto.bruno@unical.it

* Correspondence: piero.bevilacqua@unical.it

check for updates

Abstract: The use of passive solutions for building envelopes represents an important step toward the achievement of more efficient and zero-energy building targets. Trombe walls are an interesting and viable option for the reduction of building energy requirements for heating, especially in cold climates. This study presents the experimental analysis of an innovative Trombe wall configuration, named a thermo-diode Trombe wall, which was specifically designed to improve the energy efficiency by providing a proper level of insulation for the building envelope. Such a design is essential in cold climates to limit the thermal losses whilst increasing solar heat gains to the heated spaces. An experimental campaign was conducted from December to March that involved monitoring the external climatic conditions and the main thermal parameters to assess the thermal performance of the proposed solution. The results demonstrated that in the presence of solar radiation, the thermo-diode Trombe wall was able to generate significant natural convection inside the air cavity, with temperatures higher than 35 °C in the upper section, by providing consistent heat gains for the indoor environment, even on cold days and for hours after the end of the daylight. The efficiency, relative to the incident solar radiation, reached 15.3% during a well-insolated winter day.

Keywords: trombe wall; experimental analysis; solar gains; PCM thermal storage

1. Introduction

To achieve more sustainable and lower energy-consuming buildings, particular attention has been paid to the development of green standards for building construction [1]. The use of passive solutions in the building envelope appears to be more than an obligatory step. In this regard, several solutions have been proposed and studied by researchers, including green roofs [2], the Barra–Constantini system [3], the adoption of proper control strategies of venetian blinds [4], and the use of agricultural building insulating materials [5]. Trombe walls represent an interesting solution in this direction since they are capable of adequately exploiting solar energy and provide both heating and ventilation for indoor environments. In a Trombe wall, the solar radiation incident on the vertical surface is captured by an absorber with a high absorptivity coefficient. Thermal energy is stored in the Trombe wall structure thanks to the elevated thermal mass. Subsequently, thermal energy is released toward the indoor environment via air thermo-circulation, convection and long-wave radiation from the absorber inner surface. Airflow is usually activated and managed through proper vents, and it occurs in an air gap formed between an external glazed façade and the massive wall. The air in the air gap is heated and delivered to the adjacent rooms thanks to thermo-circulation, passively providing thermal energy. The massive wall is the most crucial element of a Trombe wall since it is responsible for the thermal storage [6]. Therefore, the choice of suitable materials for a massive wall is crucial as well

as the choice of an appropriate glazing system according to the climatic location [7]. The capacity of a Trombe wall to achieve energy savings has been investigated in several climatic conditions: from subtropical locations [8], to semi-arid [9] and hot Mediterranean climates [10], to cold Polish loc tions [11]. A numerical model of a Trombe wall was developed in the TRNSYS environment and validated using a small-scale experimental prototype [12], producing a 77% reduction in heating energy demand for a 16 m^2, non-insulated simple Tunisian building. In a Mediterranean location, it was found that the Trombe wall did not reduce the maximum heating load; however, an annual heating energy saving of up to 32.1% can be reached with a 37% area ratio [13]. A ventilated low-cost Trombe wall using low-tech prefab components was designed and tested for passive heating and cooling of existing buildings in Chile [14]. The results showed predicted energy savings of 44.14% and 25.35%, respectively, for two cities in different winter microclimates. More sophisticated approaches involved computational fluid dynamics (CFD) [15] for evaluating the achievable thermal performance using a Trombe wall for either a single room [16] or an entire house [17]. A three-dimensional CFD model was developed and validated to investigate a Trombe wall equipped with a venetian blind [18]. CFD was also used to investigate a composite Trombe wall, which combined a water wall and a traditional Trombe wall [19]. A building energy simulation and CFD were coupled to analyze the thermal performance of a Trombe wall with a venetian blind with the aim of regulating shading and airflow in the cavity of the solar wall in the cooling season by observing the reduction of energy consumptions [20].

Indeed, an important issue with a conventional Trombe wall is the excessive solar heat gain during summer, which can lead to indoor environments overheating by producing a worsening of the cooling requirements. Stazi et al. [21] also stressed the importance of summer shading of the Trombe wall to prevent excessive overheating and a counterproductive heat transfer to the indoor environment. The possibility of achieving summer energy savings thanks to the adoption of proper ventilation strategies was analyzed in different climatic contexts [22]. The variation of the blind tilt angle of a Trombe wall was found to have a significant effect on the limitation of cooling loads [23].

The possibility of improving the performance of a Trombe wall with appropriate modifications has been addressed by some authors. An unvented Trombe wall with an extra window in the massive wall was simulated using Solidworks in the locality of Athens, Greece, to verify the possibility of producing greater indoor temperatures and improving the internal space lighting [24]. The addition of vertical thermal fins to the internal surface was considered to improve the efficiency of an unvented Trombe wall and to maximize the heat transfer [25]. The application of vertical thermal fins on the absorber of a Trombe wall was also experimentally addressed in the arid climate of Yazd (Iran), obtaining an increase in the energy stored by up to 3% [26]. A Trombe wall, together with a solar chimney and a water spraying system, was experimentally studied in a test room under a desert climate, which resulted in enhancing the thermal efficiency by approximately 30% [27]. A novel application proposed a Trombe wall with blinds for shading and water flowing channels, obtaining a higher overall thermal efficiency [28]. An interactive glass wall, whose working principle is analogous to a Trombe wall, was presented and experimentally analyzed [29]. A modified Trombe wall prototype called a collector–accumulation wall (CAW) was experimentally assessed using a laboratory simulator to evaluate the heat distribution efficiency [30].

Some studies proposed various configurations to improve the storage capacity of the massive wall. In an experimental study of a small-scale Trombe wall, phase-change material (PCM) was inserted in the form of a brick-shaped package [31]. The integration of PCM in lightweight building components has also been considered as an important strategy to compensate for the lack of thermal storage mass of such buildings [32]. A Trombe wall integrated with a double layer of PCM wallboard on a south façade was proposed and simulated using TRNSYS software. The results showed a reduction of the peak cooling and heating loads by 9% and 15%, respectively, compared with a reference Trombe building, showing that PCM can alleviate summer overheating and maintain indoor thermal comfort like a classical Trombe building in winter [33].

In this study, we analyzed an innovative design and configuration called a thermo-diode Trombe wall (TWTD). The main feature of the proposed systems lies in the capability of providing an adequate level of thermal insulation to the building envelope that would conversely produce a strong disadvantage in common Trombe wall configurations, limiting the thermal performance. The proposed wall is characterized by a highly insulated external wall and a limited glazed surface compared to a common Trombe wall, which allows for solar radiation to be caught on the absorber surface that does not extend for the entire wall height. The heat transfer takes place due to natural convection between the lower and upper sections of the wall air gap that are established because of the peculiar configuration and thermal insulation disposition. The thermal mass is further enhanced thanks to the presence of PCM, which has been properly placed in the air cavity to prolong the passive heat gain, even after the end of the daily solar radiation.

After presenting the operating principle and the experimental set-up, the results of a monitoring campaign from December to March are reported, which demonstrates the excellent thermal behavior of the proposed system.

2. Materials and Methods

2.1. Experimental Set-Up

The experimental set-up was located at the University of Rzeszów (Poland). The study was conducted in winter in the climatic conditions of the same city. A proper heating system was able to maintain the temperature of the inside air at the desired value. During the experiments, the internal air temperature was set to 20 °C.

The TDTW apparatus in the experimental field had a total height of 2.3 m and a southern orientation (Figure 1). The system consists of two main sections. The lower zone is responsible for the absorption of solar radiation and the upper zone is responsible for heat storage and distribution. An internal air gap, developed through the entire height of the wall, connects the two sections. The thermal insulation of both sections was made of 10 cm thick expanded polystyrene. The air gap of the upper section was separated from the inside of the chamber by a 1.25 cm thick plasterboard. The glazing system consisted of a single-pane glazed unit mounted on an insulated frame. The absorber was made of a perforated black matter painted stainless-steel sheet with an absorption coefficient of 0.95, as reported in the product data sheet. Thermal properties of the TDTW materials are reported in Table 1.

Table 1. Trombe wall material and thermal properties.

| Material	Function	Thermal Conductivity (W/m·K)	Density (kg/m^3)	Specific Heat (J/kg·K)
Expanded polystyrene	Upper external insulation	0.036	20	1460
Plasterboard	Internal wall	0.17	900	1000
Expanded polystyrene	Lower internal insulation	0.036	20	1460
Stainless-steel sheet	Absorber	25	7900	460
	Type	Glass Thermal Transmittance (W/m^2·K)	Frame Thermal Transmittance (W/m^2·K)	g Value
Glazing	4/16/4	1.2	0.9	0.68
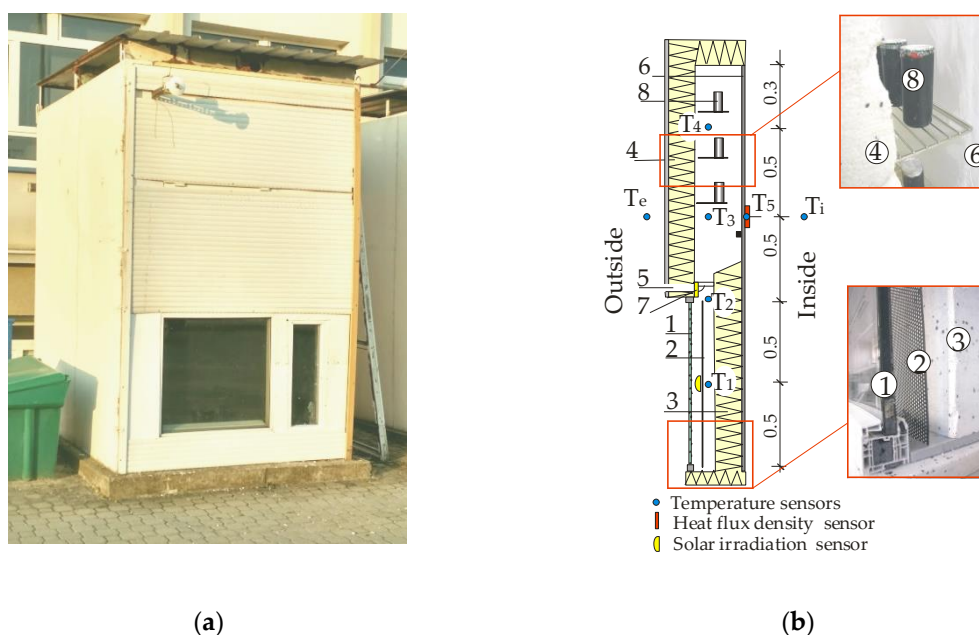
Figure 1. Scheme of the proposed thermo-diode Trombe wall (TDTW): (**a**) three-dimensional representation and (**b**) a cross-section with labels of the main components (1—glazing system, 2—black steel absorber, 3—lower insulation, 4—upper insulation, 5—vent, 6—internal wall, 7—summer mode separator, and 8—phase-change material (PCM) containers.

To increase the storage capacity of the upper section, appropriate materials with greater thermal capacities can be added. The heat can be stored during the hours of solar irradiation and then transferred to the interior of the building after sunset. Due to the high specific heat value or phase change heat, water or phase change materials (PCMs) are the most suitable materials for this function. When using a PCM, it is important to choose an appropriate melting temperature, which should correlate with the temperature range of the air heated inside the gap of the heat storage and distribution section, which accompanies the photothermal conversion of the solar radiation in the lower section of the TDTW. To increase the system's heat capacity, the storage and distribution section was equipped with five containers of 0.33 l each of PCM (RT 28, Rubitherm, Germany) placed in the middle of the height. The PCM has an enthalpy of fusion of 220–225 kJ/kg and declared melting and solidification temperatures in the range 27–29 °C.

The temperature in the air gap cavity was measured at four points at different heights. Sensors T1 to T4 were placed such that they were spaced 0.5 m from each other (Figure 1). Furthermore, the internal and external air temperature was monitored at a height of 1.5 m from the ground, while the heat flux was measured on the internal surface at approximately 1.5 m from the internal floor. The solar radiation was monitored using a sensor placed vertically in the air cavity of the lower section at a height of around 0.5 m from the ground to measure the net incident solar radiation on the absorber surface and by another sensor placed on the vertical external side of the wall at a height of 2 m. The accuracy and type of sensors used in the experiments are reported in Table 2.

Table 2. Sensors type and accuracy.

Measurement	Type	Accuracy
Temperature	ZA 9020-FS Thermo E4	±0.05 K, ±0.05% of the measured value
Heat flux density	ALMEMO FQ A020 C	<6% of the measured value
External air temperature	PT1000	±0.2 °C (−200 °C to +100 °C)
Solar irradiance	DeltaOhm LP Pyra12	<1% (first class)

The study was conducted between December and March 2019 to assess the performance of the TDTW in winter conditions.

The data were recorded every ten minutes using a 16 channels Data Acquisition System Comet MS6D. In the following analysis, the hourly averages of the data are reported and discussed for clarity of interpretation.

2.2. Winter Operating Principles

The proposed thermo-diode Trombe wall (TDTW) system exploits the thermal stratification of air and natural convection to provide thermal energy to the indoor environment. Solar radiation penetrating through the glazing located on the lower zone of the wall is absorbed on the black steel-plate absorber. The air heated by the absorber as a result of the photothermal conversion rises via natural convection, transporting heat to the top part of the wall. The heat is finally transferred to the interior room through the internal wall from the accumulation and distribution section (Figure 2).
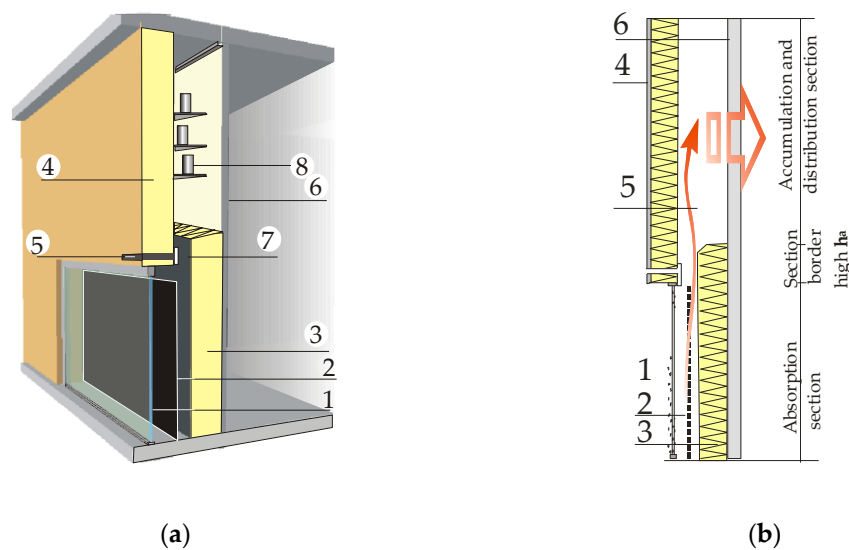

(**a**) (**b**)

Figure 2. Scheme of the proposed thermo-diode Trombe wall: (**a**) three-dimensional representation and (**b**) a cross-section, both with labels of the main components (1—glazing system, 2—black steel absorber, 3—lower insulation, 4—upper insulation, 5—vent, 6—internal wall, 7—summer mode separator, and 8—thermal storage material (PCM containers)).

In periods of low solar exposure or at night, air movement stagnation was observed due to the thermal stratification phenomenon.

To limit the heat losses, the TDTW is protected by a thermal insulation layer installed over the entire wall height but in a different position in the two sections. In the lower part, the insulation is directly placed on the internal wall, a few centimeters away from the absorber. In the upper section, the thermal insulation is placed above the glazing and constitutes the physical separation from the outside. To avoid thermal bridge effects over the border of the two sections, the bottom thermal insulation should have a height of several centimeters above the upper edge of the glazing system. This height can be initially determined by imposing a rule stating that the thermal resistance in the zone where the two insulations overlap (R_{ha}) must be equal to or greater than the thermal resistance evaluated in a perpendicular direction in each of the upper (R_{us}) and lower (R_{ls}) sections, namely:

$$R_{ha} \geq R_{us}$$
$$R_{ha} \geq R_{ls}$$

(1)

R_{ha} is the thermal resistance of the air layer at the height of the overlap of insulation h_a (m), obtainable using:

$$R_{ha} = \frac{h_a}{\lambda_a}, \tag{2}$$

where λ_a is the thermal conductivity of stagnant air (0.024 W/mK).

R_{ls} is the thermal resistance of the lower section, which is given by:

$$R_{ls} = \sum R_{si} + R_g + R_{agl} + R_{ild} + R_{wll} + R_{se}. \tag{3}$$

R_{us} is the thermal resistance of the upper section, which is given by:

$$R_{us} = \sum R_{si} + R_{agu} + R_{ilu} + R_{wlu} + R_{se}. \tag{4}$$

where:

- R_g is the thermal resistance of the glazing system;
- $R_{agl/agu}$ is the thermal resistance of the lower/upper section of the air gap;
- R_{ild}/R_{ilu} is the thermal resistance of the lower/upper section of the insulation layer;
- $R_{wll/Rwlu}$ is the thermal resistance of the lower/upper section of the wall layer;
- R_{si} and R_{se} are the surface air-wall thermal resistances.

2.3. Summer Operating Principles

The TDTW can be additionally modified to provide building cooling by exploiting the ventilation and the stack effect due to buoyancy. For this purpose, the vent duct should be connected to a solar chimney, as shown in the example in Figure 3.
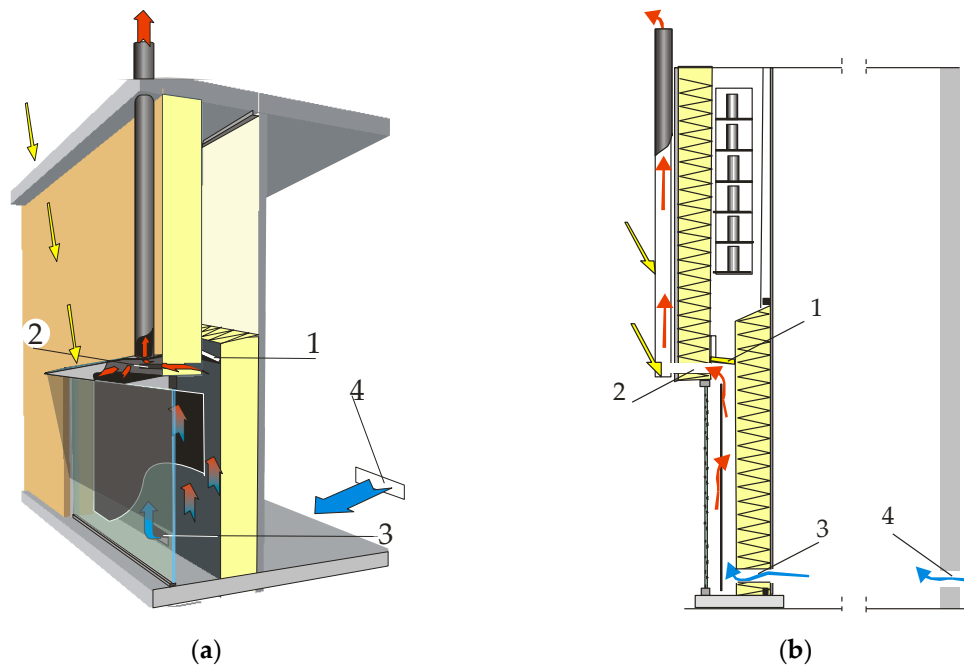

(**a**)   (**b**)

Figure 3. Diagram of the TDTW operation in summer conditions: (**a**) general view and (**b**) cross-section of the wall (1—summer flap separator, 2—vent channel, 3—lockable infiltration channel, and 4—ventilation hole located on the room of the building).

In summer, the high angle of incidences of solar radiation limit direct radiation of the glazing and absorber; however, despite this, the air in the lower absorption section can be subjected to

intense heating and consequently rise to the upper distribution zone, providing an additional load for the indoor spaces from the upper distribution section of the wall. This undesirable effect can be counteracted by using shading elements (e.g., louvers, blinds) or by using a summer mode separator flap. The rising of the flap (Figure 3) blocks the free flow of warm air and unlocks the ventilation duct, which allows for the connection of the air gap to the solar chimney. In this operational configuration, the absorber provides an increase in the air temperature of the lower section of the wall that triggers the stack effect, forcing airflow toward the external solar chimney connected to the cavity, consequently drawing a colder airflow from indoor spaces through proper vents positioned at the bottom of the internal wall.

The effectiveness of the chimney in terms of creating draft-intensifying ventilation using the TDTW in the building depends on the level of air heating in the chimney and its height. The chimney draft can be estimated using a simple relationship:

$$p_d = h_{ch} \times g \times (\rho_{ae} - \rho_{ach}) \tag{5}$$

where:

- p_d is the chimney buoyancy force (Pa);
- h_{ch} is the chimney height (m);
- g is the gravitational acceleration (m/s^2);
- ρ_{ae} is the external air density (kg/m^3);
- ρ_{ach} is the air density inside the chimney (kg/m^3).

Since the proposed TDTW was developed mainly for continental climates, the article presents and discusses the results of initial experiments conducted to assess the winter operation mode performance.

2.4. Thermal Storage Tests

A first analysis was performed to evaluate the thermal behavior and the heat storage properties of the material used in the TDTW. The study aimed to assess the heat storage capacity of PCM material placed in an aluminum can.

The main advantage of using a phase change material lies in the capacity to store heat during the melting process, therefore exploiting the latent heat of fusion of the entire container volume. To verify the heat storage capacity, the PCM cans were tested in a Memmert Humidity Chamber HCP108, with an operation range +18–160 °C and a set-point temperature accuracy of 0.1 °C, where controlled air temperatures of 30 °C, 35 °C, and 40 °C were set in three respective experiments. The experiments aimed at reproducing the real operation conditions of the can in the TDTW; indeed, these temperatures expected in the Trombe wall air cavity when solar radiation is available. The temperature was measured and recorded at intervals of 1 min. Four temperature sensors distributed along the radius were used to measure the radial temperature profile (Figure 4).
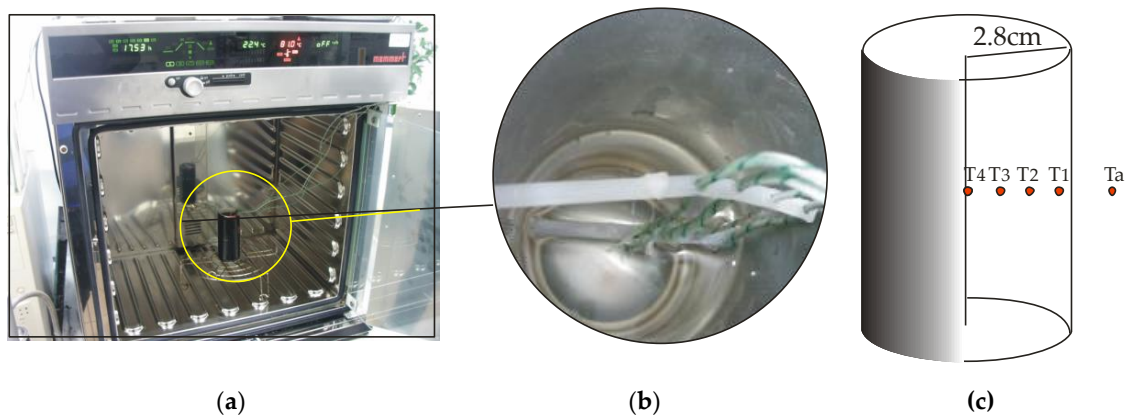
| (a) | (b) | (c) |

Figure 4. (**a**) Memmert climatic chamber, (**b**) top view of cans with liquefied PCM and temperature sensors, and (**c**) temperature sensor distribution in the container.

3. Results and Discussion

3.1. Thermal Storage Capacity of the PCM Containers

The temperatures found during the three tests are reported in Figure 5. Considering the test with a chamber temperature of 30 °C (Figure 5a), it was possible to observe the behavior of the PCM material. As soon as the chamber was activated, the air temperature jumped to the set-point value of 30 °C. As a consequence, the PCM started to warm rapidly with the most external sensor (T1) increasing before the others placed in the inner part of the container. When T1 reached a value of about 23 °C, a sudden variation of the curve slope was observed, denoting the beginning of the melting process, and when it finished, the temperature increase was much slower. When a value of 26 °C was reached, there was another sudden slope variation, where the temperature increased with the same rate as the initial phase until the achievement of the set-point value imposed by the chamber. It is interesting to observe that when the melting front reached the most external sensor (T4), all the curves overlapped, indicating a uniform temperature distribution due to the liquid phase. When the chamber was turned off, the air temperature swiftly fell to a value of around 20 °C. Consequently, the PCM followed the rapid decline just as quickly until all the sensors registered a value of around 24.5 °C. Then, an abrupt change of slope was observed in the curves, where they tended to be almost flat, denoting, in this case, the start of the solidification process. It is possible to observe that the most external part of the container, being directly subject to the cooling effect of the chamber air, was the first to complete the solidification, with its temperature that started to decrease while the other parts were still completing the phase change.

Similar trends were observed when setting the chamber temperature to 35 °C (Figure 5b) and 40 °C (Figure 5c).

In light of the obtained results, it is possible to define the effective contribution of PCM in thermal storage as the period between the time of the discontinuity in the temperature curve during the cooling process and the time when the most external sensor T4 deviates from the other curves (which denotes complete solidification of the PCM container). In the three tests, the discharge period was found to be in the range of 3.98 h to 4.22 h, confirming the positive contribution that the use of such a material can provide in the proposed TDTW.
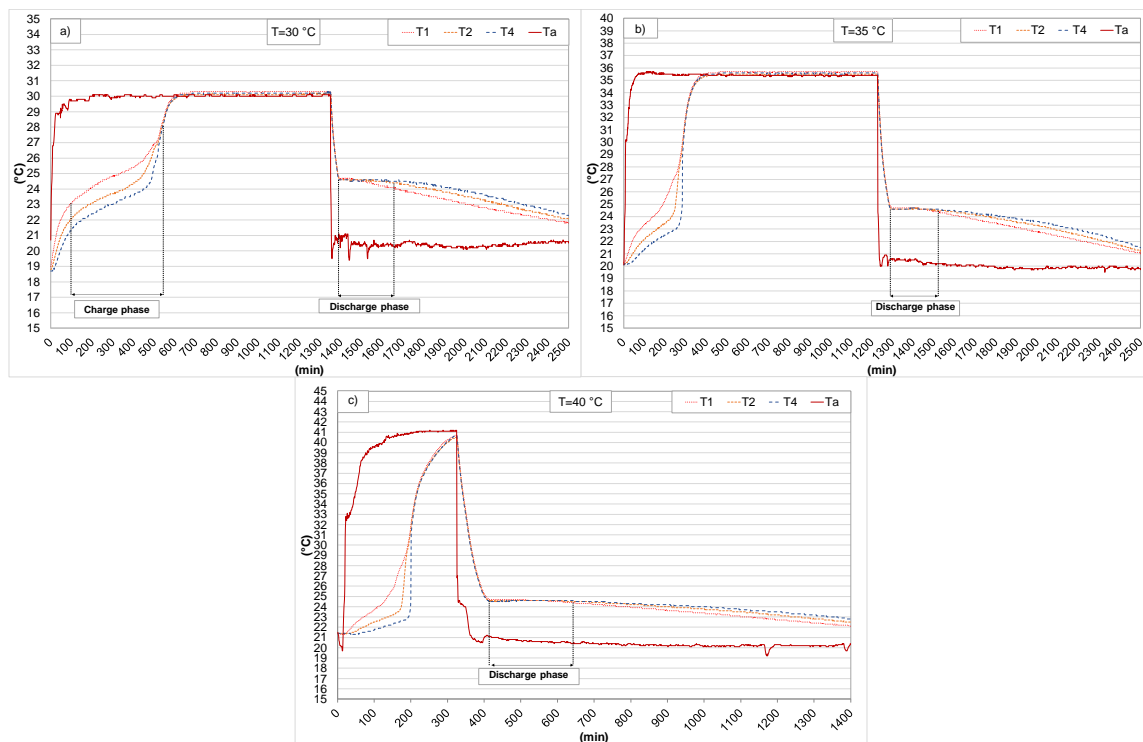
Figure 5. Temperature measurements along the radial direction of the PCM container during the tests on the climatic chamber with set-point temperatures of 30 °C (**a**), 35 °C (**b**), and 40 °C (**c**).

3.2. Analysis in Clear-Sky Conditions

To assess the performance of the proposed TDTW, Figure 6 represents the monitoring of variables over three days (17–19 February 2019), which were characterized by clear-sky conditions with the presence of solar radiation for almost the entire daylight period. In these conditions the registered external temperatures were low, varying from 1.1 °C to 16.4 °C, without falling below 0 °C. It must be highlighted that the solar radiation shown in the following graphs was recorded using the sensor placed in the air cavity of the lower section of the wall, and therefore represents the amount of radiation that struck the absorber after being transmitted by the glazed surface. The daily peak of solar radiation ranged between 335.4 W/m^2 and 375.5 W/m^2, with a distinct daily pattern that is typical of clear-sky conditions. The indoor environment was kept at 20 °C via the climatic chamber operation.

A similar daily pattern appeared for the monitored variables for all three days. For the first day, during the night, the air gap in the lower section of the Trombe wall (T1 and T2) showed low temperatures because of the great thermal exchanges toward the outdoor environment throughout the glazed surface. As soon as the solar radiation appeared, the temperature rose abruptly, with T1 growing from 6.5 °C to a peak of 45.2 °C at 13:00, and T2 followed a similar trend. The solar radiation transmitted through the glazed surface was absorbed by the black steel absorber that consistently heated the air in the cavity's lower section. The increase in air temperature produced an intensification of natural convection inside the air cavity by consequently heating the upper section of the wall. This can be seen by observing temperatures T3 and T4, which registered peaks of 38.9 °C and 38.4 °C, respectively, at 14:00, with one hour of time lag compared to the peak temperature of the bottom section.
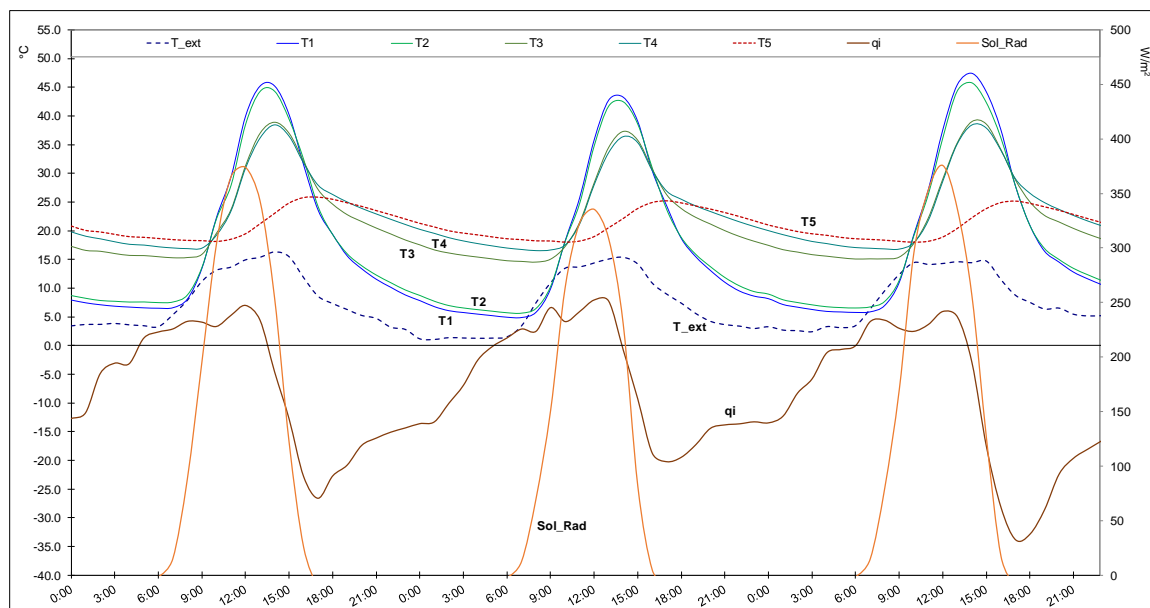
Figure 6. Solar radiation (Sol_Rad), external air temperature (T_ext), air gap temperature (T1, T2, T3, T4), indoor surface temperature (T5), and heat flux (qi) for 17–19 February 2019 (Sol_Rad and qi on the right *y*-axis, temperature on the left *y*-axis).

After sunset, because of the greater thermal losses toward the external environment, T1 and T2 dropped swiftly to reach a daily minimum value that was below 10 °C. The effect produced by the PCM containers was more interesting: it enabled the heat produced by natural convection to be stored in the upper cavity (T3 and T4) during the peak temperature hours and then release it for a prolonged time (up to 4 h, as demonstrated in Figure 5). It can be seen from Figure 6 that because of the heat released by the PCM containers during the solidification process, the upper section cavity temperatures (T3 and T4) decreased with a lower slope, with T4 remaining higher than T3, as a result of the presence of the PCM.

The heat flux was positive, indicating a net loss of thermal energy for the indoor environment, from early morning (04:30) until 13:30. After this time, an inversion of heat flux occurred, denoting net thermal energy entering the indoor spaces, until the late afternoon (17:30). Then, the heat flux reversed again in the early morning of the following day. The same daily cycle was repeated for the next two days.

The results clearly show how the proposed Trombe Wall generated heat gains that shifted in time after the end of the daylight hours, with a positive contribution until the first hours of the morning. The peak entering heat flux of 26.6 W/m^2, as an absolute value, was found at 17:00.

It must be highlighted that the greater temperature values in the cavity upper section were also attributable to the heat flux from the conditioned indoor space that provided heat to the cavity (when a positive heat flux was observed). Yet, the positive effect of the proposed Trombe wall, with staggered and alternating thermal insulation in the two sections, allowed the upper cavity temperature to not fall below 15 °C. The results also showed that the thermal energy lost through the internal wall toward the air cavity (36.0 Wh/m^2 for the first day) was considerably lower, as an absolute value, than the thermal energy provided to the indoor spaces (207.7 Wh/m^2 for the same day). The other two days repeated almost the same trends of the examined variables.

A further interesting aspect is the behavior of the wall in the presence of solar radiation but with a much colder external temperature for 22–23 February 2019, as reported in Figure 7. The solar radiation still reached a peak of 398.1 W/m^2 on 22 February and a peak of 332.1 W/m^2 on 23 February, but the air temperature dropped considerably, reaching minimum values of −5.1 °C and −7.0 °C, respectively, and daily peaks of 4.9 °C and 3.3 °C respectively.
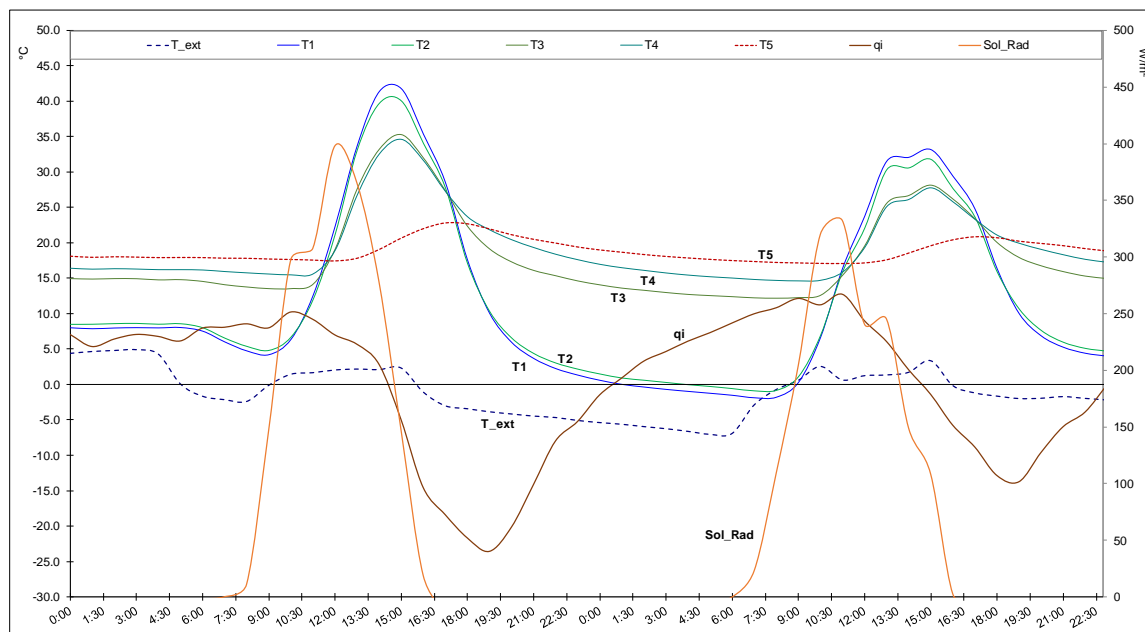
Figure 7. Solar radiation (Sol_Rad), external air temperature (T_ext), air gap temperature (T1, T2, T3, T4), indoor surface temperature (T5), and heat flux (qi) for 22–23 February 2019 (Sol_Rad and qi on the right *y*-axis, temperature on the left *y*-axis).

In this scenario, the TWTD was still able to generate high temperatures in the air cavity, even though the lower solar radiation recorded in the second monitored day produced markedly lower temperature levels. From Figure 7, it is evident how the Trombe wall was able to increase the air cavity temperature, even after the solar radiation peak. On 22 February, T1 started from a value of 8.0 °C and rapidly increased to reach a peak of 41.8 °C at 15:00, with T2 following the same trend with a slightly lower peak value. It then decreased as swiftly as it rose, falling to values close to 0 °C at midnight because of the consistent drop of the external temperature and the consequent thermal losses through the glazed surface. Nevertheless, the cold external air did not prevent the possibility of reaching high temperatures in the upper section of the cavity, where T3 (and T4 being close) reached a value of 35.3 °C due to the natural convection triggered by the lower cavity. As a result, the heat flux inverted at the time of the temperature peak, showing that thermal energy was provided to the indoor spaces until the end of the day. For the whole day, the heat gains amounted to 130 Wh/m^2 against thermal losses of 106.2 Wh/m^2. Furthermore, it is possible to appreciate how the presence of PCM material in the upper cavity of the wall produced a more stable temperature (both T3 and T4), which declined with a low gradient. The heat flux registered a peak of 23.6 W/m^2 at 19:00.

On 23 February, the lower available solar radiation induced a lower temperature in the air gap: in the lower section T1 reached 33.2 °C, whereas in the upper section, a maximum of 28.2 °C was attained by T5, again at 15:00. Despite the colder outdoor temperature and lower solar radiation, the TDTW was still able to generate positive heat gains with a heat flux that inverted at 15:00, similar to the previous day, showing that thermal energy was transferred toward the indoor space. The heat gains amounted to 63.7 Wh/m^2, lower than the 104.9 Wh/m^2 lost toward the air cavity.

3.3. Analysis in Overcast Sky Conditions

Since the main driving force of a Trombe wall is the solar radiation that is converted and transferred toward the indoor spaces, it is important to verify the thermal behavior of the proposed TDTW in overcast conditions, which can often occur in winter. The results in Figure 8 show the trend of the monitored variables for two overcast days in February (21/02/2019 and 24/02/2019).
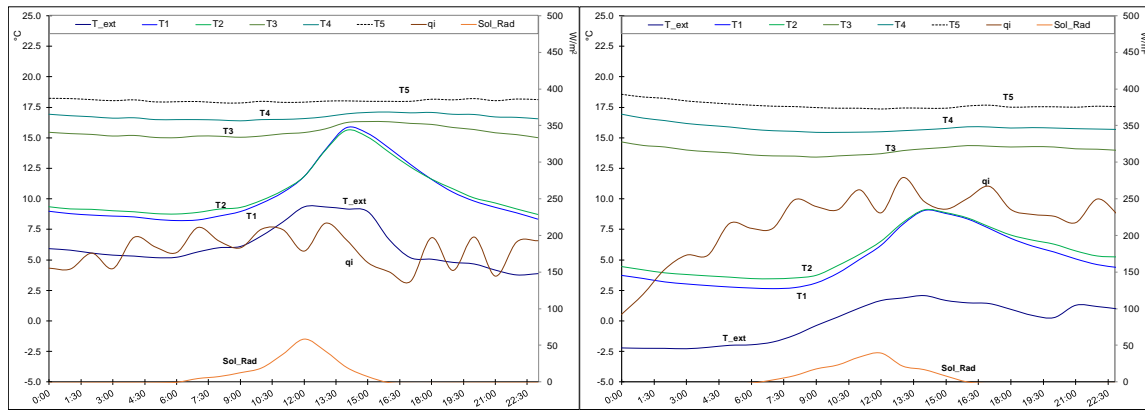
Figure 8. Solar radiation (Sol_Rad), external air temperature (T_ext), air gap temperature (T1, T2, T3, T4), indoor surface temperature (T5), and heat flux (qi) for 21 February 2019 (**left**) and 24 February 2019 (**right**) (Sol_Rad and qi on the right *y*-axis, temperature on the left *y*-axis).

The scarce amount of solar radiation, which reached a peak of 58.7 W/m^2 on 21 February and 39.1 W/m^2 on 24 February, was not sufficient to activate the passive heating of the internal space. On 21 February (Figure 8 on the left), the lower section of the cavity was not able to reach a proper temperature to adequately transfer heat in the upper section via natural convection, with T1 showing a modest peak of 15.8 °C. T3 and T4 showed a rather stable trend around their mean values of 15.5 °C and 16.7 °C, respectively, during the whole day. Even the indoor surface temperature was fairly stable around its mean value of 18.0 °C. In this condition, the upper section TDTW temperature was mainly produced by the heat flux coming from indoor spaces through the internal wall. A similar situation was observed on 24 February (Figure 8 on the right), where because of the more stringent temperatures, T1 in the lower section did not rise above 9.1 °C. T3 and T4 again showed a stable trend around their mean values of 14.0 °C and 15.8 °C, respectively, whereas T5 showed an almost flat curve around its mean of 17.7 °C.

As already observed for the clear-sky conditions, an evident correlation between thermal flux and external air temperature appeared. When the average external air temperature was 6.1 °C (on 21 February) the registered heat flux peak was 8.0 W/m^2, with a total daily thermal energy loss of 138.9 Wh/m^2; with an average external air temperature of −0.1 °C (on 24 February), the registered heat flux peak was 11.7 W/m^2, with a total daily thermal energy loss of 193.5 Wh/m^2.

3.4. Trombe Wall Efficiency

To assess the overall winter performance of the proposed TWTD system, Table 3 reports the daily summary of the main monitored variables for the whole period of the experimental campaign. The daily efficiency of the Trombe wall η_d was determined using:

$$\eta_d = \frac{rQ_{gain}}{Q_{sol}} = \frac{r \int \left| q_i^- \right| dt}{\int \varphi \, dt}, \tag{6}$$

where:

- φ is the solar irradiation available on the TWTD absorption surface (W/m^2);
- q_i^- is the heat flux entering the conditioned space through the internal wall (W/m^2);
- r is the ratio between the distribution area A_d that provides heat flux to the indoor spaces to the external glazing area A_g that receives the solar radiation. The integrals are performed over the entire day considered.

Table 3. Cumulative daily solar irradiation on the wall's surface, average external air temperature, thermal energy leaving the indoor room through the internal, and the thermal efficiency of the proposed TWTD.

Date	Rad_sol (Wh/m^2)	T_ext,ave (°C)	Thermal Loss (Wh/m^2)	Efficiency (-)
15 Feb	360.6	5.2	178.5	0.0%
16 Feb	4316.6	6.3	129.9	8.7%
17 Feb	4639.4	7.9	36.0	12.0%
18 Feb	3962.2	6.9	42.3	12.8%
19 Feb	4621.4	8.0	31.5	15.3%
20 Feb	1266.2	6.3	46.3	9.4%
21 Feb	516.2	6.1	138.2	0.0%
22 Feb	4643.8	−0.1	105.3	7.6%
23 Feb	3961.3	−2.0	107.0	4.5%
24 Feb	448.1	−0.1	193.8	0.4%
25 Feb	2896.7	5.5	148.2	5.8%
26 Feb	3163.0	7.2	69.1	7.4%
27 Feb	2315.1	6.0	58.3	5.9%
28 Feb	3722.4	10.4	51.8	7.4%
1 Mar	2499.2	4.0	49.8	9.7%

As seen in Table 3, the TDTW was only unable to provide heat gains in severe weather conditions with a low amount of daily solar irradiation, where the entering heat flux was not registered. Nevertheless, the amount of thermal energy leaving the indoor space toward the air cavity (maximum of 193.8 Wh/m^2 on 24 February) was not consistently greater than the amount registered in the days of normal operation of the Trombe wall. The efficiency reached a maximum of 15.3% on 19 February, a greatly insolated day. The higher availability of solar radiation produced higher efficiencies; however a correlation with the external air temperature also appeared. With the same solar irradiation, the efficiency grew with the daily average air temperature: considering 17, 19, and 22 February, with similar levels of daily solar irradiation (4639.4 Wh/m^2, 4621.4 Wh/m^2, and 4643.8 Wh/m^2, respectively), the efficiency grew from 7.6% to 12.0% when the average air temperature increased from −0.1 °C to 7.9 °C, and reached a maximum of 15.3% for a temperature of 8.0 °C. A significant slump in efficiency from 12.8% to 4.5% was observed when the air temperature dropped from 6.9 °C to −2.0 °C with a similar level of solar irradiation (3962.2 Wh/m^2 and 3961.3 Wh/m^2 on 18 and 23 February, respectively).

It must be noted that the performance of the wall was evaluated in cold winter conditions. It is possible to assume, based on the results obtained, that in intermediate seasons, where there is a non-negligible demand of energy for space heating in the particular climate condition, the TDTW can reach even greater efficiency and produce higher heat gains for indoor spaces.

4. Conclusions

To reach the target of sustainable and lower energy-consuming buildings, the adoption of proper technical solutions for the envelope appears to be a necessary step. The use of passive systems, such as Trombe walls, can generate important heat gains by converting the solar radiation striking the absorbing surface into thermal energy that is available for heating requirements. Especially in cold climates, the scarce availability of solar radiation can often lead to the adoption of highly insulated envelopes, limiting the exploitable solar gains. To combine the effects of a high-thermal-resistance wall and convert the available solar radiation into a positive heat gain, a new Trombe wall concept, called a thermo-diode Trombe wall, was proposed. An experimental campaign conducted in winter allowed for analysis of the thermal behavior of the system in different meteorological conditions. The use of PCM as a thermal storage material proved to be an interesting solution since preliminary tests conducted in a climatic chamber demonstrated the capacity of the containers to release heat during the solidification process for a period of 4 h when subject to typical temperatures reached in the Trombe wall.

The results of the analysis demonstrated the capability of the TDTW to trigger consistent natural convection, producing temperatures in the air cavity that exceeded 35 °C on winter days with available solar radiation. For a clear-sky day, the thermal energy provided to the indoor room was 207.7 Wh/m^2 compared with the 36.0 Wh/m^2 lost toward the air cavity. Even on cold days, the system was able to convert solar radiation and produce considerable benefits for the conditioned room, with a heat gain of 130 Wh/m^2 compared with a thermal loss of 106.2 Wh/m^2. There were only a few days where an almost negligible solar radiation was registered and the TDTW was unable to generate positive heat gains, but being highly insulated meant the thermal losses toward the external environment were constant.

When comparing days with similar solar radiation, the efficiency was found to increase with the daily average external air temperature. The maximum efficiency of 15.3% was produced on a day with solar irradiation of 4621.4 Wh/m^2 and an average external air temperature of 8.0 °C.

Finally, the analysis demonstrated that the proposed system represents an important solution to improve the thermal efficiency of the buildings, leading to the realization of the nZEB concept, especially in cold climates where a highly insulated envelope is important.

5. Patents

Szyszka, J. and Lichołai, L., Rzeszow University of Technology, A collector–accumulative barrier; patent application 21.02.2019 r. nr PL.428996 (in the Polish language).

References

1. Telichenko, V.; Benuzh, A.; Eames, G.; Orenburova, E.; Shushunova, N. Development of Green Standards for Construction in Russia. *Procedia Eng.* **2016**, *153*, 726–730. [CrossRef]
2. Bevilacqua, P.; Bruno, R.; Arcuri, N. Green roofs in a Mediterranean climate: Energy performances based on in-situ experimental data. *Renew. Energy* **2020**, *152*, 1414–1430. [CrossRef]
3. Imessad, K.; Messaoudene, N.A.; Belhamel, M. Performances of the Barra-Costantini passive heating system under Algerian climate conditions. *Renew. Energy* **2004**, *29*, 357–367. [CrossRef]
4. Nicoletti, F.; Carpino, C.; Cucumo, M.A.; Arcuri, N. The Control of Venetian Blinds: A Solution for Visual Comfort. *Energies* **2020**, *13*, 1731. [CrossRef]
5. Cascone, S.M.; Cascone, S.; Vitale, M. Building insulating materials from agricultural by-products: A review. In *Sustainability in Energy and Buildings*; Springer: Berlin/Heidelberg, Germany, 2020.
6. Hami, K.; Draoui, B.; Hami, O. The thermal performances of a solar wall. *Energy* **2012**, *39*, 11–16. [CrossRef]
7. Koyunbaba, B.K.; Yilmaz, Z. The comparison of Trombe wall systems with single glass, double glass and PV panels. *Renew. Energy* **2012**, *45*, 111–118. [CrossRef]
8. Krüger, E.; Suzuki, E.; Matoski, A. Evaluation of a Trombe wall system in a subtropical location. *Energy Build.* **2013**, *66*, 364–372. [CrossRef]
9. Dabaieh, M.; Elbably, A. Ventilated Trombe wall as a passive solar heating and cooling retrofitting approach; a low-tech design for off-grid settlements in semi-arid climates. *Sol. Energy* **2015**, *122*, 820–833. [CrossRef]
10. Soussi, M.; Balghouthi, M.; Guizani, A. Energy performance analysis of a solar-cooled building in Tunisia: Passive strategies impact and improvement techniques. *Energy Build.* **2013**, *67*, 374–386. [CrossRef]
11. Błotny, J.; Nemś, M. Analysis of the Impact of the Construction of a Trombe Wall on the Thermal Comfort in a Building Located in Wrocław, Poland. *Atmosphere* **2019**, *10*, 761. [CrossRef]
12. Abbassi, F.; Dimassi, N.; Dehmani, L. Energetic study of a Trombe wall system under different Tunisian building configurations. *Energy Build.* **2014**, *80*, 302–308. [CrossRef]
13. Jaber, S.; Ajib, S. Optimum design of Trombe wall system in mediterranean region. *Sol. Energy* **2011**, *85*, 1891–1898. [CrossRef]

14. Agurto, L.; Allacker, K.; Fissore, A.; Agurto, C.; De Troyer, F. Design and experimental study of a low-cost prefab Trombe wall to improve indoor temperatures in social housing in the Biobío region in Chile. *Sol. Energy* **2020**, *198*, 704–721. [CrossRef]

15. Bajc, T.; Todorović, M.N.; Svorcan, J. CFD analyses for passive house with Trombe wall and impact to energy demand. *Energy Build.* **2015**, *98*, 39–44. [CrossRef]

16. Abdeen, A.; Serageldin, A.A.; Ibrahim, M.G.E.; El-Zafarany, A.; Ookawara, S.; Murata, R. Experimental, analytical, and numerical investigation into the feasibility of integrating a passive Trombe wall into a single room. *Appl. Therm. Eng.* **2019**, *154*, 751–768. [CrossRef]

17. Shashikant, K.N. Numerical analysis of house with trombe wall. *Int. Res. J. Eng. Technol.* **2016**, *3*, 966.

18. Hong, X.; He, W.; Hu, Z.; Wang, C.; Ji, J. Three-dimensional simulation on the thermal performance of a novel Trombe wall with venetian blind structure. *Energy Build.* **2015**, *89*, 32–38. [CrossRef]

19. Zhou, L.; Huo, J.; Zhou, T.; Jin, S. Investigation on the thermal performance of a composite Trombe wall under steady state condition. *Energy Build.* **2020**, *214*, 109815. [CrossRef]

20. Hong, X.; Leung, M.K.H.; He, W. Effective use of venetian blind in Trombe wall for solar space conditioning control. *Appl. Energy* **2019**, *250*, 452–460. [CrossRef]

21. Stazi, F.; Mastrucci, A.; di Perna, C. Trombe wall management in summer conditions: An experimental study. *Sol. Energy* **2012**, *86*, 2839–2851. [CrossRef]

22. Bevilacqua, P.; Benevento, F.; Bruno, R.; Arcuri, N. Are Trombe walls suitable passive systems for the reduction of the yearly building energy requirements? *Energy* **2019**, *185*, 554–566. [CrossRef]

23. Hu, Z.; He, W.; Hong, X.; Ji, J.; Shen, Z. Numerical analysis on the cooling performance of a ventilated Trombe wall combined with venetian blinds in an office building. *Energy Build.* **2016**, *126*, 14–27. [CrossRef]

24. Bellos, E.; Tzivanidis, C.; Zisopoulou, E.; Mitsopoulos, G.; Antonopoulos, K.A. An innovative Trombe wall as a passive heating system for a building in Athens—A comparison with the conventional Trombe wall and the insulated wall. *Energy Build.* **2016**, *133*, 754–769. [CrossRef]

25. Abbassi, F.; Dehmani, L. Experimental and numerical study on thermal performance of an unvented Trombe wall associated with internal thermal fins. *Energy Build.* **2015**, *105*, 119–128. [CrossRef]

26. Rabani, M.; Rabani, M. Heating performance enhancement of a new design trombe wall using rectangular thermal fin arrays: An experimental approach. *J. Energy Storage* **2019**, *24*, 100796. [CrossRef]

27. Rabani, M.; Kalantar, V.; Dehghan, A.A.; Faghih, A.K. Empirical investigation of the cooling performance of a new designed Trombe wall in combination with solar chimney and water spraying system. *Energy Build.* **2015**, *102*, 45–57. [CrossRef]

28. Hu, Z.; Zhang, S.; Hou, J.; He, W.; Liu, X.; Yu, C.; Zhu, J. An experimental and numerical analysis of a novel water blind-Trombe wall system. *Energy Convers. Manag.* **2020**, *205*, 112380. [CrossRef]

29. Szyszka, J. Experimental evaluation of the heat balance of an interactive glass wall in a heating season. *Energies* **2020**, *13*, 632. [CrossRef]

30. Szyszka, J. Simulation of modified Trombe wall. In Proceedings of the VII Conference SOLINA, Polańczyk, Poland, 19–23 June 2018.

31. Zalewski, L.; Joulin, A.; Lassue, S.; Dutil, Y.; Rousse, D. Experimental study of small-scale solar wall integrating phase change material. *Sol. Energy* **2012**, *86*, 208–219. [CrossRef]

32. Fiorito, F. Trombe walls for lightweight buildings in temperate and hot climates. Exploring the use of phase-change materials for performances improvement. *Energy Procedia* **2012**, *30*, 1110–1119. [CrossRef]

33. Zhu, N.; Li, S.; Hu, P.; Lei, F.; Deng, R. Numerical investigations on performance of phase change material Trombe wall in building. *Energy* **2019**, *187*, 116057. [CrossRef]